the FEBS Journal
MINIREVIEW

Nucleosome-remodelling machines and other molecular motors observed at the single-molecule level

Christophe Lavelle[1,2], Elise Praly[3], David Bensimon[3], Eric Le Cam[2] and Vincent Croquette[3]

1 Genome Dynamics and Regulation, Muséum National d'Histoire Naturelle, CNRS UMR 7196/INSERM U565, Paris, France
2 Molecular Microscopies and Genome Maintenance, Institut Gustave Roussy, CNRS UMR 8126/Univ Paris Sud, Villejuif, France
3 LPS, Ecole Normale Supérieure, CNRS UMR 8550, Paris, France

Keywords
atomic force microscopy; electron microscopy; helicases; magnetic tweezers; molecular motors; nucleosomes; optical tweezers; remodelling factors; single molecule

Correspondence
Christophe Lavelle, CNRS UMR 7196/INSERM U565, Muséum National d'Histoire Naturelle, 43 rue Cuvier, 75005 Paris, France
Fax: +33 0(1) 40 79 37 05
Tel: +33 (0)1 40 79 48 32
E-mail: lavelle@mnhn.fr
Vincent Croquette, LPS/CNRS UMR 8550, Ecole Normale Supérieure, 24 rue Lhomond, 75231 Paris Cedex 05, France
Fax: +33 0(1) 44 32 34 33
Tel: +33 (0)1 44 32 34 92
E-mail: vincent.croquette@lps.ens.fr

(Received 28 March 2011, revised 15 June 2011, accepted 12 July 2011)

doi:10.1111/j.1742-4658.2011.08280.x

Through its capability to transiently pack and unpack our genome, chromatin is a key player in the regulation of gene expression. Single-molecule approaches have recently complemented conventional biochemical and biophysical techniques to decipher the complex mechanisms ruling chromatin dynamics. Micromanipulations with tweezers (magnetic or optical) and imaging with molecular microscopy (electron or atomic force) have indeed provided opportunities to handle and visualize single molecules, and to measure the forces and torques produced by molecular motors, along with their effects on DNA or nucleosomal templates. By giving access to dynamic events that tend to be blurred in traditional biochemical bulk experiments, these techniques provide critical information regarding the mechanisms underlying the regulation of gene activation and deactivation by nucleosome and chromatin structural changes. This minireview describes some single-molecule approaches to the study of ATP-consuming molecular motors acting on DNA, with applications to the case of nucleosome-remodelling machines.

Introduction

DNA is associated *in vivo* with histones to form chromatin fibers, the repetitive unit of which, the nucleosome, consists of 147 bp of DNA wrapped around an octamer containing two copies of the four core histones H2A, H2B, H3 and H4 [1]. This packaging, which leads to compaction and topological deformation of the DNA [2], is dynamic to allow transient access of regulatory proteins to DNA. Part of the dynamics is mediated by chromatin-remodelling factors (thereafter called remodellers) that use the energy of ATP hydrolysis to facilitate the interaction of proteins with nucleosomal DNA [3–9]. These large complexes are characterized by the presence of an ATPase subunit from the sucrose non-fermentation 2 (Snf2) family of

Abbreviations
3D, three dimensional; AFM, atomic force microscopy; TEM, transmission electron microscopy; OT, optical tweezers; MT, magnetic tweezers.

the helicase-like superfamily, SF2 [10,11]. Remodellers may therefore share similarities with other molecular motors, such as helicases or translocases, in their mechanisms of action.

Remodellers have been linked to various biological functions but not much is known about how they operate *in vivo* [12]. Remodelling reactions range from sliding of histones relative to DNA, exchange of histone components or complete dissociation of histones, therefore respectively altering the position, structure or presence of the nucleosome [11,13,14]. Although remodellers have been extensively studied by various approaches *in vitro*, many questions remain as to the precise mechanism(s) of remodelling and as to the possible exploitation of spontaneous nucleosome fluctuations [15].

Single-molecule approaches have recently complemented conventional biochemical and biophysical techniques to decipher the complex mechanisms that rule chromatin dynamics [16–19]. While atomic force microscopy (AFM) backs up electron microscopy to scrutinize DNA–protein interactions at the atomic scale [20–22], magnetic and optical tweezers enable the measurement of forces and torques produced by molecular motors acting on DNA or chromatin templates [23–25]. These novel approaches provide us with new insights into chromatin remodelling performed by ATP-consuming machines [26,27]. In this review, we will describe some of the techniques used to visualize and manipulate single molecules and discuss how studying remodellers acting on DNA, along with other molecular motors, such as translocases and helicases, can enlighten our understanding of remodelling mechanisms.

Visualizing DNA-interacting enzymes

Two main devices are currently used to look at biological samples with molecular resolution: transmission electron microscopes and atomic force microscopes. Transmission electron microscopy (TEM) uses high-velocity electron beams with an associated wavelength of about a nanometer. It involves the acceleration of electrons by a high voltage difference and the focusing of these electrons by electromagnetic lenses. The beam passes through the specimen before it reaches the imaging system of the microscope [fluorescent screen, photographic plate or light-sensitive sensor such as a charge-coupled device (CCD) camera] (Fig. 1A). As most biological materials are nearly transparent to electrons, specimens are usually shadowed by tungsten or stained using heavy metals, such as uranium, to scatter imaging electrons and enhance the contrast between different structures (Fig. 2A,B). By enabling

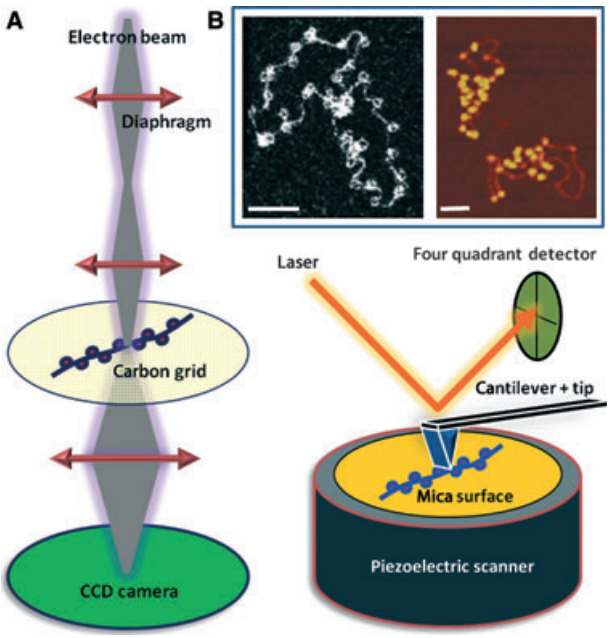

Fig. 1. Molecular microscopy: the two main devices. (A) Transmission electron microscopy (TEM) and (B) atomic force microscopy (AFM) both enable the visualization of nucleoprotein complexes at a nanometric scale. Insert: TEM (left) and AFM (right) images of nucleosomal arrays reconstituted with purified histones on bacterial plasmids (scale bars = 50 nm).

preservation of the specimen in a snapshot of its solution state through cryofixation [rapid freezing of a specimen so that the water forms vitreous (noncrystalline) ice], cryo-electron microscopy (cryo-TEM) has emerged as a powerful technique to observe frozen samples in their fully hydrated three-dimensional (3D) structure. However, the lack of staining or shadowing has to be compensated by sophisticated image analysis and reconstruction. Macromolecular structures can also be obtained by 3D reconstruction from collections of TEM-negative staining pictures. Use of such a technique recently provided a low-resolution structure of several remodellers [28–31]. Readers interested in this technique will have a better idea of how electron microscopy enables 3D reconstruction of macromolecular complexes by looking at dedicated reviews on the subject [32]. 3D reconstruction is not discussed here as our intention is to focus exclusively on techniques pertaining to the direct visualization of chromatin and other DNA–protein complexes [33,34].

The atomic force microscope is another type of high-resolution imaging device, although the term 'microscope' is actually misleading because the information is gathered by 'feeling' the sample rather than by 'looking' at it (Figs 1B and 2C). The atomic force

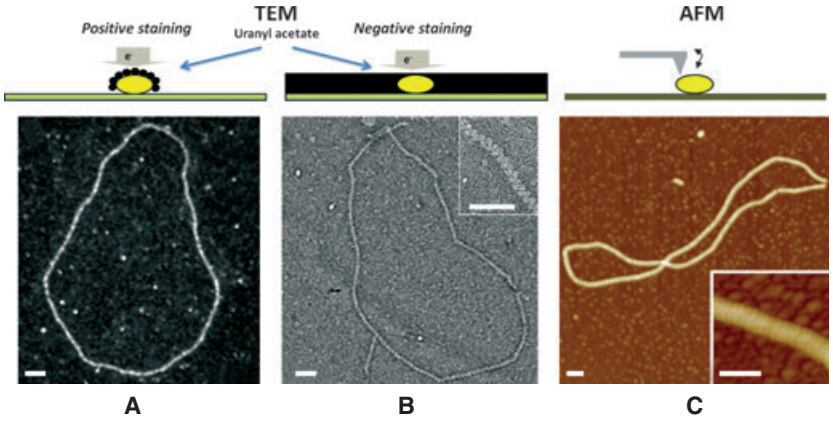

Fig. 2. Imaging of nucleoprotein complexes: different techniques for different information. A Rad51 filament formed on a circular dsDNA plasmid is visualized under three different conditions. (A) TEM operated in darkfield mode: the molecules are stained with uranyl acetate (positive staining); this technique provides a good contrast. (B) TEM operated in brightfield mode: the whole grid is covered with uranyl acetate (negative staining); this technique allows the filament to be seen in more detail (e.g. distinguishing its chirality). (C) AFM in air; no need for staining, and one can still count every gyre of the filament. All scale bars = 50 nm.

microscope consists of a cantilever with a sharp tip (probe) at its end that scans the specimen surface. When the probe comes into proximity with the surface, the forces between the tip and the sample lead to a deflection of the cantilever, measured using a laser beam reflected from the top of the cantilever on a four-quadrant photodiode. A feedback mechanism is usually employed to adjust the tip-to-sample distance to maintain a constant force between the tip and the sample. For this, the sample is mounted on a piezoelectric tube, moving the sample in the z direction to maintain a constant force and in the x and y directions to scan the sample [35]. Bustamante (partly in collaboration with our laboratory [36]), Hansma and colleagues pioneered its uses as a tool to visualize DNA [36–39] and nucleosomes [40–43]. In comparison with TEM, one of the biggest advantages of AFM is to enable imaging in solution, which not only gives access to DNA and proteins in their 'natural' environment (opening the door to affinity studies with functionalized probes [27,44]) but also provides opportunities for real-time dynamic studies. Note that even when imaging is carried out in air, the sample stays in wet conditions, hence preserving its native structure. Also, it enables continuous multiscale observation (from DNA to mitotic chromosome) [45–47] without any fixation/coloration.

Feeling DNA-interacting enzymes

Single-molecule manipulation techniques appear as sensitive and versatile tools to study molecular mechanisms [23–25,48,49]. In typical experiments, one investigates DNA or nucleosomal templates one-at-a-time, either by applying physical forces and measuring subsequent deformation of the substrate or by using DNA as a mechanosensor to measure DNA–protein interactions [16,17]. Magnetic tweezers (MT) and optical tweezers (OT) use a microscopic bead to manipulate a single molecule in order to deduce useful biological information. The position of the bead labelling the molecule's extremity can be measured with nanometre resolution, giving access to extension changes comparable to a few base pairs on DNA. To reach this accuracy, the single molecule must be stretched to reduce its Brownian fluctuations. This is achieved either by magnetic forces (MT) or by electromagnetic forces (OT) (Fig. 3A,B) [49].

OT are constructed by focusing a laser beam very tightly with a microscope objective (Fig. 3A). A transparent bead whose refractive index is higher than the surrounding medium is affected by the force exerted by the refracted beam. As a result it ends up at the focal point of the electromagnetic field where the optical forces on the bead cancel out. The bead is thus trapped in a potential well that tightly follows the trap position. This device allows for manipulating the bead in 3D with extreme accuracy. Such a device is a position clamp: one sets the trap's position. Small deviations of the bead from that point result in an optical force that counterbalances an external force (e.g. the force exerted by a motor pulling on a DNA anchored to the bead).

MT consist of a pair of macroscopic magnets placed at a controlled distance above the sample (Fig. 3B).

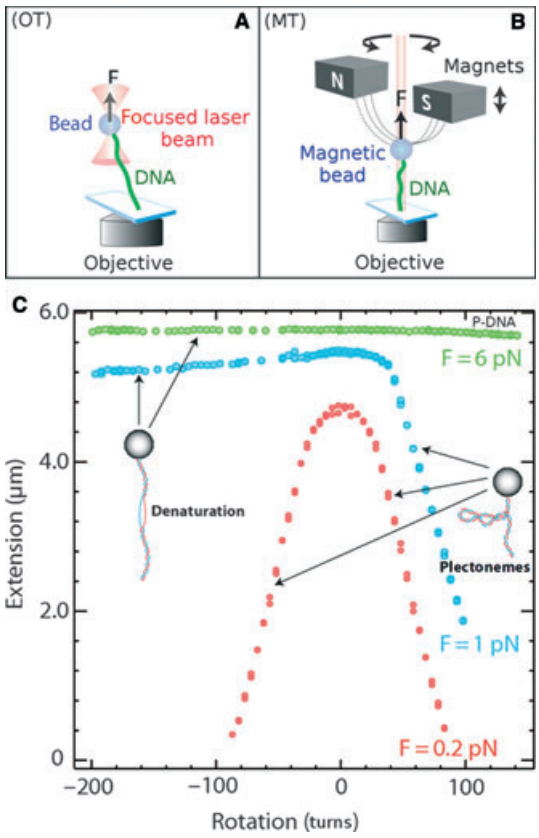

Fig. 3. Tweezers: the two main devices. (A) In optical tweezers (OT), a laser beam is focused by a microscope objective producing a region of high electromagnetic field trapping polystyrene or silica beads. (B) In magnetic tweezers (MT), two magnets produce a strong horizontal magnetic field with a strong vertical gradient which pull the magnetic bead upwards. In both situations the bead is tethered to the surface by a DNA molecule. (C) Torsonial behavior of a DNA molecule at different stretching forces: at low force (red curve), the DNA buckles (shortening of the molecule as a result of the formation of plectonemes upon writhing) whenever the molecule is twisted in one direction or in the other so that the extension versus rotation curve is symmetrical. When the force is increased (blue curve), torque increases and the curve becomes asymmetrical; supercoils still form for positive coiling while local denaturation relieves the torsional stress for negative constraints. At larger forces (green curve), no plectonemes are observed, even on positively supercoiled DNA: the torsional stress is absorbed in local structural change of the molecule [denaturation in (–) and P-DNA in (+)].

They produce a strong magnetic field gradient that exerts typically a vertical force on a magnetic bead. This force is constant over the distance spanned by the magnetic bead (a few microns) and its magnitude can be controlled with the distance separating the magnets from the beads (a few millimetres). The position of the bead is tracked in real-time by video microscopy. MT work in force clamp mode as one imposes the force and measures the resulting molecule's extension [24]. As a result of their simple architecture, MT are one of the most popular and widespread biophysical techniques [24]. They were first used to handle a single DNA molecule and measure its elasticity [50] and response to torsion [51], before being more recently applied to study single nucleosomal arrays [52–55]. MT indeed provide a powerful technique to test the response of chromatin fibers to physiological levels of tension and/or torsion (recently and quite exhaustively reviewed [17]). MT offer a very simple way to control the torsional state of a dsDNA molecule: by rotating the magnets while keeping them at a constant distance from the beads, one rotates the magnetic beads and twists the DNA (provided that the molecule is not free to rotate, i.e. not nicked and anchored at multiple points at its ends). When twisted, the molecule may form torsional loops or plectonemes, as also seen on twisted ropes. As these structures appear, the molecule shortens significantly (Fig. 3C). At constant force, past a certain threshold this shortening is linear with the number of coils (e.g. the number of rotations of the magnets) [56]. Taking advantage of this nice feature, one can, for instance, record in real time the torsional relaxation achieved by topoisomerases cycle after cycle [57].

The intrinsic noise limitation of both techniques is related to the dissipation of the probe (fluctuation dissipation theorem), which is related to the viscous drag on the bead: the smaller the bead, the smaller the drag and the better the signal-to-noise ratio. However, reducing the size of the bead limits the maximal force (F_m) that can be applied, which scales as its volume: for both OT and MT the size of the bead is limited to about one micron for the F_m to be $\sim$ 20 pN [48]. MT and OT appear as complementary tools and offer the ability to study tensional and torsional constraints on the molecule. With MT, rotating the magnetic field direction offers a very simple way to twist a molecule from a well-defined angle (angular clamp) [58]. With OT, torsion is also possible although at the expense of a more complex set up as one needs to rotate the polarization of the trapping beam. However, by tracking the change of polarization produced by the bead, one can deduce the torque applied on the molecule (torque clamp) [59].

Over the past few years, several single-molecule studies have addressed the properties of individual nucleic acid-associated motor proteins [60,61] including remodellers [17,26]. It is indeed tempting to suppose that translocases, helicases and remodellers share similarities in their mechanisms of action. As stressed by Flaus and Owen-Hugues, Snf2 family ATPases are also found in organisms where no nucleosome exists, which

suggests that their DNA-dependent translocase activity does not act on the nucleosome alone [11]. We review below some recent observations obtained in our laboratories from visualization and/or manipulation of single DNA (or nucleosomal) substrates subjected to molecular motors and remodeller actions, and provide, at the same time, a quick overview of related works in the field.

Watching and catching DNA-interacting enzymes in the act

MT and OT are well adapted for studying DNA molecular motors, as these enzymes travel along DNA molecules, often altering their shape and hence modifying the DNA extension in a specific way and leading to a detectable signal. One of the most studied molecular motors is the helicase, which typically translocates along one strand of a DNA duplex stripping off the second strand in a zipper fashion. An ideal template to study helicases consists of a DNA-hairpin attached at one end to a surface and at the other end to a bead. At small forces (not enough to unzip the molecule) the DNA has minimal extension and presents a dsDNA fork under tension. As a helicase loads onto the fork and starts unwinding the hairpin, the molecule is unzipped and its extension is increased: each separated base-pair increases the extension by about 0.8 nm (Fig. 4A) [62]. Such small enzymes are usually difficult to be directly visualized on DNA, but image analysis and reconstruction from negative-staining picture collections can provide a good view of their structure [63]. However, what can be directly visualized is the dramatic action of helicases on DNA–protein complexes, such as Rad51 filaments. Rad51 protein is a well-known protagonist of homologous recombination in eukaryotic cells, along with various mediators [64]. Like RecA in bacteria and RadA in Archaea, Rad51 promotes an ATP-mediated strand-exchange reaction by polymerizing on DNA and forming a helical filament. As seen in Fig. 4B, such a Rad51–ssDNA nucleoprotein filament is quickly destabilized (< 2 min) when incubated with 100 nm of the Srs2 helicase [65].

TEM and AFM are, in fact, great tools with which to visualize how proteins – including molecular motors – interact with DNA and the potential role of ATP in the process. Recently, such an approach enabled us to evidence the remodelling capacity of Rad51, revealing a new remodelling mechanism performed by a 'noncanonical remodeller' (e.g. a recombinase) [66] (Fig. 5). Rad51 has indeed been reported to polymerize on ssDNA as well as on dsDNA [67,68], raising the question of how this polymerization takes place in the

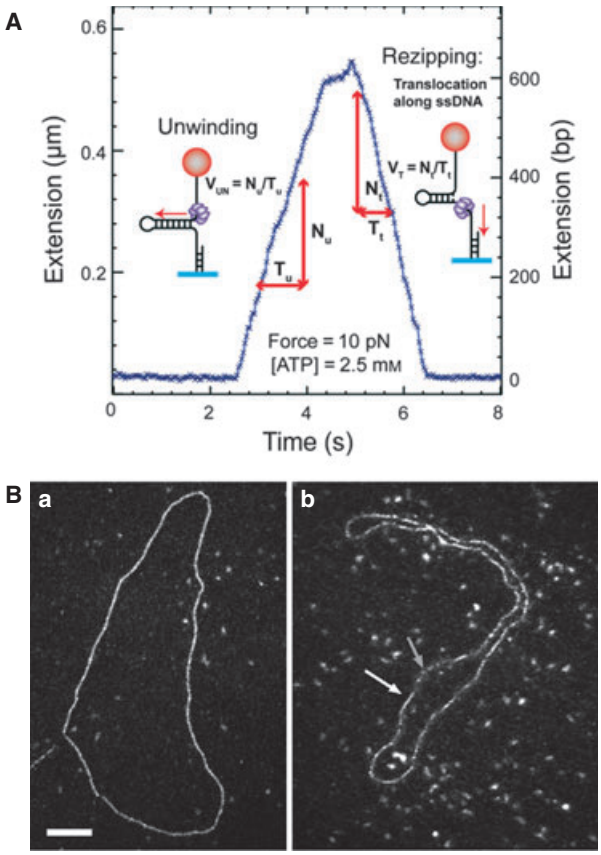

Fig. 4. Helicase properties investigated by tweezers and molecular imaging. (A) Helicase-unwinding event observed on a DNA hairpin. The replicative helicase gp41 encircles one strand of the DNA molecule and pumps this strand through the hole of its hexameric shape. By doing so the enzyme strips off the second strand, producing an increase in the molecule extension. When the enzyme passes the hairpin apex, it refolds in the back of the enzyme which now travels along the ssDNA. The refolding of the hairpin reduces the molecule extension revealing the distance spanned by the enzyme. (B) Helicases such as gp41 are too small to be seen on DNA using a standard TEM-positive staining technique. However, the action of helicases on DNA–protein complexes, such as Rad51 filaments, can lead to dramatic effects easily visualized by TEM, as seen from this image: a Rad51–ssDNA nucleoprotein filaments (a) is quickly destabilized when incubated with helicase Srs2 (b) (the white arrow shows intact Rad51 nucleoprotein filament and the grey arrow indicates regions of destabilized filament; scale bar = 200 nm; images from [65]).

context of chromatin. Rad51 polymerization on dsDNA has been extensively studied by MT [69–71], but its action on nucleosome potentially sitting on this DNA had never been addressed. Our quantitative analyses by TEM and AFM clearly demonstrated the occurrence of chromatin remodelling upon nucleoprotein filament formation: during Rad51 polymerization; recombinase proteins moved mononucleosomes as well

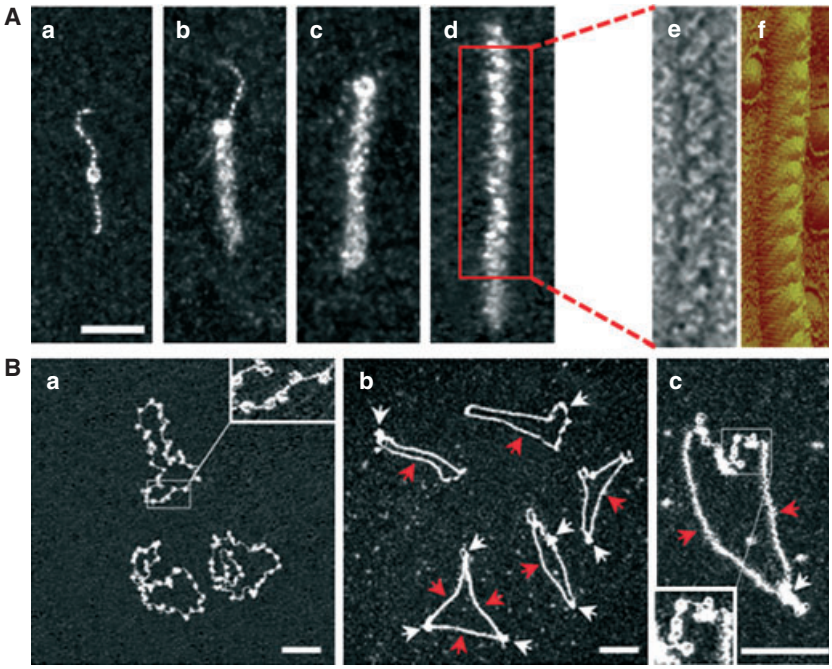

Fig. 5. Nucleosome remodelling by a recombinase. Some enzymes not known as remodellers still have the capability to displace nucleosomes 'on the run', as is the case for Rad51 recombinase. (A) Nucleosomes were reconstituted on a 601 positioning sequence located at the center of a 347-bp DNA fragment. Despite the high stability of these nucleosomes, Rad51 polymerization shifts and even ejects nucleosomes out of the DNA template (a–d; scale bar = 50 nm). (e,f) Zoom on the filament by negative staining (e) and AFM (f). (B) Nucleosomal arrays were reconstituted on PhiX174 supercoiled plasmids (a; inset: enlarged image of nucleosomes). When Rad51 is added, two to three filaments are generally formed (from two to three nucleation sites, probably starting in the linker DNA between nucleosomes), stretching over several hundred base pairs on straight nucleosome-free DNA and pushing nucleosomes into two to three dense arrays. (b,c; red and white arrows show Rad51 filament and nucleosome clusters, respectively; inset: enlarged image of nucleosomes compacted by Rad51 filament). Scale bars = 100 nm; images from [66].

as whole nucleosomal arrays in front of the progressing filament, stressing the powerful remodelling capacity of Rad51 (Fig. 5). Similar behavior was observed with RecA (although no histones are encountered in bacteria, various sets of proteins compact DNA [72]), opening up new possibilities for understanding DNA recombination and revealing new types of ATP-dependent chromatin dynamics [66].

Other DNA-interacting proteins have been shown to behave as remodeller-like enzymes and disrupt chromatin structure in the course of their action: RNA polymerases, of course (reviewed in [73,74]), but also DNA-repair enzymes, such as hMSH2/6 [75], the *Escherichia coli* motor protein, RuvAB [76], or the *E. coli* RecBCD and simian virus 40 (SV40) large T-antigen helicases [77,78]. Conversely, remodellers exhibit properties, such as processive ATP-driven translocation along DNA, that are characteristic of DNA helicases. One difficulty encountered in the study of remodellers (compared with other DNA-translocating machines) is related to their relevant physiological molecular substrate (i.e. chromatin). While dsDNA displays a fairly well-understood and characterized behavior upon stretching and twisting [79], chromatin fibers appear to be far less reproducible and their elastic behavior is still the subject of intense investigation and debate (see [16,17] and references therein). Several reasons explain this situation: different protocols exist for chromatin fiber reconstruction, which do not give the same results; the fiber is relatively fragile and tensional or torsional constraints may alter its integrity; finally, nucleosomes exist with different components or degrees of methylation or acetylation, possibly leading to different mechanical properties. Lacking a reliable chromatin reference state makes it more difficult to detect the possible changes in that state as a result of remodelling.

Looking at 'canonical' remodellers

The first single-molecule observations of DNA translocation by a remodeller were performed in our labora-

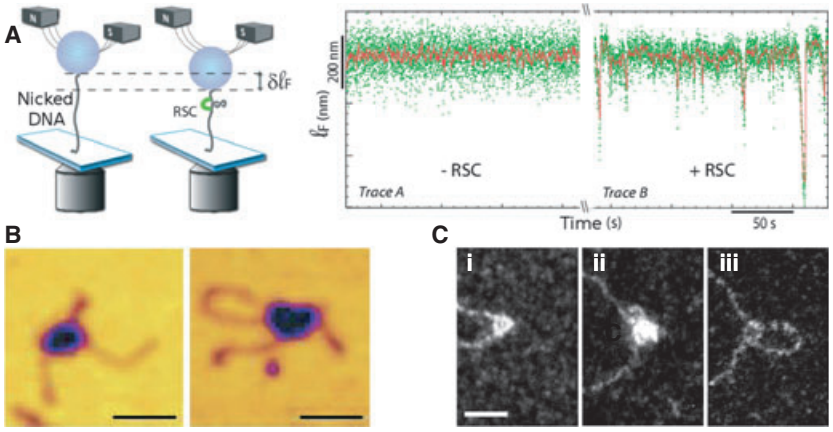

Fig. 6. RSC properties investigated by tweezers and molecular imaging. (A) The DNA extension (l_F) is monitored at a fixed force ($F \sim 0.3$ pN) and [ATP] ~100 mM. Binding of RSC to DNA decreases its extension, as seen from the time traces of the variation in the DNA extension in the absence of RSC (Trace A) and in the presence of RSC (Trace B) (raw data [green] and averaged over 1 s [red]) [80]. (B) AFM images of RSC–DNA complexes; note the presence of a (relaxed or supercoiled) loop associated with the complex (bar = 50 nm; images taken from [80]). (C) TEM images of nucleosomes before (i), during (ii) and after (iii) interaction with RSC (bar 40 nm), highly suggestive of the capability of RSC to transiently unfold DNA from the histone surface (images taken from [102]).

tory [80]. Using MT with naked DNA, we observed, at forces < 1 pN, that a single remodells the structure of chromatin (RSC) complex could cause transient shortening of the DNA as a result of the formation of a negatively supercoiled loop (Fig. 6). Many enzymes are able to form a DNA loop with a defined size δl. Such a topological structure actually shortens the extension of a dsDNA molecule, leading to an easily detectable signal in a single-molecule assay [81]. Typically, one stretches a dsDNA molecule under constant force, F_s, while recording its extension. Whenever a looping event occurs, the extension abruptly decreases by the size of the loop δl. The DNA stretching force is a very useful control parameter because increasing this force favors the unlooped state. At a well-defined F_s value, the looped and unlooped states have equal free energy and the molecule will spontaneously fluctuate between the two states. Its extension thus displays a typical telegraphic random signal (Fig. 6A).

In parallel with these studies, the group of Carlos Bustamante used OT to monitor the action of both RSC and switching/sucrose non-fermenting (SWI/SNF) complexes on single nucleosomes in real time [82]. This group worked at forces of > 3 pN in order to avoid loop formation on bare DNA; in this way they could study the translocase activity specifically related to nucleosome remodelling in isolation. Their set up gives access to the physical parameters associated with translocation except for the twist, namely speed, force and processivity. Amazingly, these two studies differed quite remarkably in their measurements of RSC translocation properties, including velocity (> 200 vs. 13 bp·s^{-1}), processivity (700 vs. 100 bp) and stalling force (1 vs. 12 pN). To add to the confusion, a recent study of the activity of a minimal RSC translocase motor (comprising the RSC ATPase subunit Sth1 and the two actin-related proteins Arp7 and Arp9) on bare DNA provides a new, different set of paremeters (e.g. a processivity of 35 bp, a velocity of 25 bp·s^{-1} and a stalling force of > 30 pN) [83]. These differences could arise from the experimental set up (MT vs. OT) or the components (DNA vs. nucleosomal substrate, full vs. minimal RSC complex); further studies should help to resolve these discrepancies.

At the same time, the group of Michelle Wang used a sophisticated 'unzipping' technique to analyse single nucleosome products following remodelling by SWI/SNF [84]. The general mechanism that emerges from these single-molecule studies is a 'DNA inchworm' model involving both twist and loop propagation (~ 1 bp of twist for 10 bp of translocation) [26]. This model explains why the displacements after remodelling that are measured by Wang's group are much smaller than the loop sizes measured by the other two groups [80,82]. Indeed, the inchworm-like action of both DNA-binding domains generates large loops that are likely to be resorbed substantially before imparting DNA translocation. As a result, the displacements are expected to be much smaller than the loop sizes or, more precisely, the loop is formed by repetitive displacements until a slippage releases the loop. The former observations that RSC can transiently

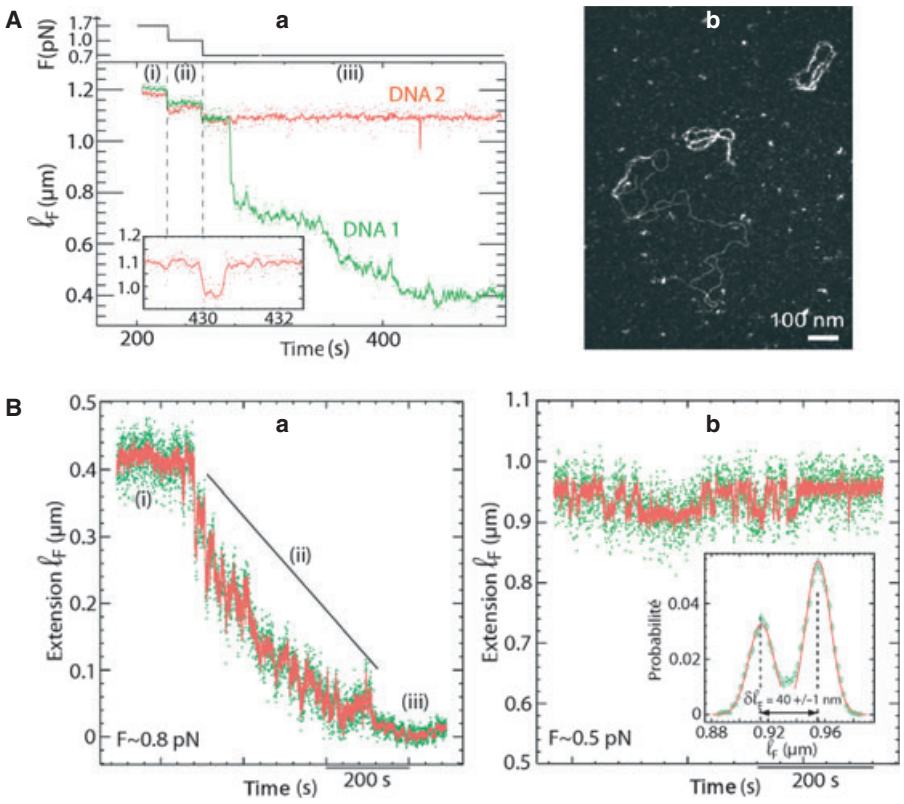

Fig. 7. Isw1a and CHD1 ATP-independent action on naked DNA. (A) Illustration of the cooperative binging of Isw1a to naked DNA (in the absence of ATP). (a) While the force (F) is controlled (upper continuous trace), the resulting extension of the molecules is recorded. At F = 1.7 pN (trace i) and F = 1.0 pN (trace ii), the two beads show restricted Brownian fluctuations about a mean value that varies with the stretching force. At 0.7 pN (trace iii), while the length of the DNA bound to bead 2 (DNA2) is unchanged (except for a quick transient decrease at ~ 430 s enlarged in the inset), the DNA anchored to bead 1 (DNA1) exhibits a rapid decrease in extension. (b) Representative TEM observations of a 4-kb linear DNA incubated with Isw1a. DNA collapse is observed on some DNA molecules in the presence of Isw1a, while naked DNA molecules are still present; scale bar = 100 nm [94]. (B) (a) Recording of the end-to-end extension of a DNA molecule in the presence of CHD1 (without ATP) at 0.8 pN. The extension of the molecule decreases rapidly owing to the cooperative binding of multiple CHD1 complexes until the bead reaches the surface of the capillary and remains stuck on it (see the decrease in amplitude of the Brownian motion of the bead). (b) In very-low-concentration conditions, one can record isolated binding/unbinding events as shown in this figure: the binding of one CHD1 complex decreases the DNA extension by 40 ± 1 nm. The presence of ATP does not modify these observations [94].

unravel nucleosome [85], trigger its translocation [86] and potentially let it in a persistently altered form [87] are consistent with the various pictures obtained by TEM and AFM (Fig. 6B) and fit the 'remosome' model proposed by Dimitrov and colleagues [88]. The same kind of scenario has emerged from studies on the related SWI-SNF remodeller, also shown to creates loops, as seen on polynucleosomes in TEM [89] and AFM [90–92], and to alter nucleosome–DNA contact in a 'remosome-like' intermediate structure [93].

In a continuation of these investigations and with an approach similar to that used to study the RSC complex, we have recently studied the behavior of yet another class of remodellers: the yeast complexes yeast imitation switch 1a (yIsw1a) and yeast chromodomain helicase DNA binding protein 1 (yCHD1). In contrast to RSC, which displayed isolated bursts of ATP-dependent DNA-translocation activity, both enzymes exhibit strong ATP-independent binding cooperativity on bare DNA [94, 95] (Fig. 7). This cooperative binding appears as an ATP-independent molecular bridging mechanism where the two pieces of bare DNA escaping a nucleosome are strongly coupled by several remodellers in a 'tank chain' structure. ATP then activates the translocation activity of these enzymes, which displace the nucleosome [95]. How this striking cooperativity actually participates in chromatin remodelling *in vivo* has still to be related to X-ray structural data recently obtained by Richmond and colleagues with yISW1a lacking its ATPase domain [96].

Conclusions

Observing the activity of chromatin remodelling factors is not an easy task: one of the major issues concerns the fact that the chromatin fiber is not a simple substrate, and its stability and intrinsic elastic properties are not simply characterized by merely measuring its extension at a given force. We believe that adding new information to the usual elastic behavior in OT or MT should help resolve this issue. Clearly, fluorescence information – in particular fluorescence resonance energy transfer (FRET) –, coupled with OT and MT systems, should help to better characterize the activities of the chromatin remodellers. At the same time, many efforts should also be made towards the extraction, characterization and manipulation of native chromatin fibers [97–99], or even *in vivo* single-molecule manipulation studies [100,101]. Regarding molecular visualization techniques, both their spreading (bench low-voltage TEM, cheaper and more user-friendly AFM) and improvement (high-speed and liquid AFM) should bring a collection of new data adding fresh molecular insights into remodelling mechanisms.

Acknowledgements

We deeply thank all our collaborators who participated in this work, especially Pauline Dupaigne, Olivier Piétrement and Anne de Cian. We also apologize to all of our colleagues whose work could not be cited here as a result of the unreachable exhaustiveness regarding such an emancipating field. D.B. acknowledges the support of an EU MolMachine grant and ANR FarC.

References

1 Luger K, Mader AW, Richmond RK, Sargent DF & Richmond TJ (1997) Crystal structure of the nucleosome core particle at 2.8 A resolution. *Nature* **389**, 251–260.
2 Prunell A (1998) A topological approach to nucleosome structure and dynamics: the linking number paradox and other issues. *Biophys J* **74**, 2531–2544.
3 Becker PB & Horz W (2002) ATP-dependent nucleosome remodeling. *Annu Rev Biochem* **71**, 247–273.
4 Lusser A & Kadonaga JT (2003) Chromatin remodeling by ATP-dependent molecular machines. *Bioessays* **25**, 1192–1200.
5 Eberharter A & Becker PB (2004) ATP-dependent nucleosome remodelling: factors and functions. *J Cell Sci* **117**, 3707–3711.
6 Clapier CR & Cairns BR (2009) The biology of chromatin remodeling complexes. *Annu Rev Biochem* **78**, 273–304.
7 Gangaraju VK & Bartholomew B (2007) Mechanisms of ATP dependent chromatin remodeling. *Mutat Res* **618**, 3–17.
8 Hargreaves DC & Crabtree GR (2011) ATP-dependent chromatin remodeling: genetics, genomics and mechanisms. *Cell Res* **21**, 396–420.
9 Bowman GD (2010) Mechanisms of ATP-dependent nucleosome sliding. *Curr Opin Struct Biol* **20**, 73–81.
10 Flaus A, Martin DM, Barton GJ & Owen-Hughes T (2006) Identification of multiple distinct Snf2 subfamilies with conserved structural motifs. *Nucleic Acids Res* **34**, 2887–2905.
11 Flaus A & Owen-Hughes T (2011) Mechanism for ATP dependent remodelling: the means to the end. *Febs J* **278**, 3579–3595.
12 Erdel F & Rippe K (2011) ISWI chromatin remodelers in mammalian cells - where, when and why? *Febs J* **278**, 3608–3618.
13 Flaus A & Owen-Hughes T (2004) Mechanisms for ATP-dependent chromatin remodelling: farewell to the tuna-can octamer? *Curr Opin Genet Dev* **14**, 165–173.
14 Saha A, Wittmeyer J & Cairns BR (2006) Chromatin remodelling: the industrial revolution of DNA around histones. *Nat Rev Mol Cell Biol* **7**, 437–447.
15 Blossey R & Schiessel H (2011) The dynamics of the nucleosome: thermal effects, external forces, and ATP. *Febs J* **278**, 3619–3632.
16 Chien FT & van Noort J (2009) 10 years of tension on chromatin: results from single molecule force spectroscopy. *Curr Pharm Biotechnol* **10**, 474–485.
17 Lavelle C, Victor JM & Zlatanova J (2010) Chromatin fiber dynamics under tension and torsion. *Int J Mol Sci* **11**, 1557–1579.
18 Zlatanova J & Leuba SH (2003) Chromatin fibers, one-at-a-time. *J Mol Biol* **331**, 1–19.
19 Zlatanova J & Leuba S (2004) Chromatin structure and dynamics: lessons from single molecule approaches. In *Chromatin Structure and Dynamics: State-of-the-Art* (Zlatanova J & Leuba S eds), pp. 369–396. Elsevier, Amsterdam.
20 Bazett-Jones DP & Eskiw C (2004) Chromatin structure and function: lessons from imaging techniques. In *Chromatin Structure and Dynamics: State-of-the-Art* (Zlatanova J & Leuba S eds), pp 343–368. Elsevier, Amsterdam.
21 Lyubchenko YL & Shlyakhtenko LS (2009) AFM for analysis of structure and dynamics of DNA and protein-DNA complexes. *Methods* **47**, 206–213.
22 Bustamante C & Rivetti C (1996) Visualizing protein-nucleic acid interactions on a large scale with the scanning force microscope. *Annu Rev Biophys Biomol Struct* **25**, 395–429.
23 Bustamante C, Cheng W & Meija YX (2011) Revisiting the central dogma one molecule at a time. *Cell* **144**, 480–497.

24 Meglio A, Praly E, Ding F, Allemand JF, Bensimon D & Croquette V (2009) Single DNA/protein studies with magnetic traps. *Curr Opin Struct Biol* **19**, 615–622.
25 Zlatanova J & van Holde K (2006) Single-molecule biology: what is it and how does it work? *Mol Cell* **24**, 317–329.
26 Cairns BR (2007) Chromatin remodeling: insights and intrigue from single-molecule studies. *Nat Struct Mol Biol* **14**, 989–996.
27 Lohr D, Bash R, Wang H, Yodh J & Lindsay S (2007) Using atomic force microscopy to study chromatin structure and nucleosome remodeling. *Methods* **41**, 333–341.
28 Asturias FJ, Chung WH, Kornberg RD & Lorch Y (2002) Structural analysis of the RSC chromatin-remodeling complex. *Proc Natl Acad Sci U S A* **99**, 13477–13480.
29 Leschziner AE, Saha A, Wittmeyer J, Zhang Y, Bustamante C, Cairns BR & Nogales E (2007) Conformational flexibility in the chromatin remodeler RSC observed by electron microscopy and the orthogonal tilt reconstruction method. *Proc Natl Acad Sci U S A* **104**, 4913–4918.
30 Skiniotis G, Moazed D & Walz T (2007) Acetylated histone tail peptides induce structural rearrangements in the RSC chromatin remodeling complex. *J Biol Chem* **282**, 20804–20808.
31 Smith CL, Horowitz-Scherer R, Flanagan JF, Woodcock CL & Peterson CL (2003) Structural analysis of the yeast SWI/SNF chromatin remodeling complex. *Nat Struct Biol* **10**, 141–145.
32 Sorzano CO, Jonic S, Cottevieille M, Larquet E, Boisset N & Marco S (2007) 3D electron microscopy of biological nanomachines: principles and applications. *Eur Biophys J* **36**, 995–1013.
33 Fisher HW & Williams RC (1979) Electron microscopic visualization of nucleic acids and of their complexes with proteins. *Annu Rev Biochem* **48**, 649–679.
34 Griffith JD & Christiansen G (1978) Electron microscope visualization of chromatin and other DNA-protein complexes. *Annu Rev Biophys Bioeng* **7**, 19–35.
35 Lyubchenko YL (2011) Preparation of DNA and nucleoprotein samples for AFM imaging. *Micron* **42**, 196–206.
36 Vesenka J, Guthold M, Tang CL, Keller D, Delaine E & Bustamante C (1992) Substrate preparation for reliable imaging of DNA molecules with the scanning force microscope. *Ultramicroscopy* **42–44** (Pt B), 1243–1249.
37 Bustamante C, Vesenka J, Tang CL, Rees W, Guthold M & Keller R (1992) Circular DNA molecules imaged in air by scanning force microscopy. *Biochemistry* **31**, 22–26.
38 Hansma HG, Vesenka J, Siegerist C, Kelderman G, Morrett H, Sinsheimer RL, Elings V, Bustamante C & Hansma PK (1992) Reproducible imaging and dissection of plasmid DNA under liquid with the atomic force microscope. *Science* **256**, 1180–1184.
39 Li MQ, Hansma HG, Vesenka J, Kelderman G & Hansma PK (1992) Atomic force microscopy of uncoated plasmid DNA: nanometer resolution with only nanogram amounts of sample. *J Biomol Struct Dyn* **10**, 607–617.
40 Leuba SH, Yang G, Robert C, Samori B, van Holde K, Zlatanova J & Bustamante C (1994) Three-dimensional structure of extended chromatin fibers as revealed by tapping-mode scanning force microscopy. *Proc Natl Acad Sci U S A* **91**, 11621–11625.
41 Yang G, Leuba SH, Bustamante C, Zlatanova J & van Holde K (1994) Role of linker histones in extended chromatin fibre structure. *Nat Struct Biol* **1**, 761–763.
42 Zlatanova J, Leuba SH, Yang G, Bustamante C & van Holde K (1994) Linker DNA accessibility in chromatin fibers of different conformations: a reevaluation. *Proc Natl Acad Sci U S A* **91**, 5277–5280.
43 Vesenka J, Hansma HG, Siegerist C, Siligardi G, Schabtach E & Bustamante C (1992) Scanning force microscopy of circular DNA and chromatin in air and propanol. *SPIE* **1639**, 127–137.
44 Wang H, Bash R & Lohr D (2007) Two-component atomic force microscopy recognition imaging of complex samples. *Anal Biochem* **361**, 273–279.
45 Fritzsche W, Schaper A & Jovin TM (1994) Probing chromatin with the scanning force microscope. *Chromosoma* **103**, 231–236.
46 Iwabuchii S, Mori T, Ogawa K, Sato K, Saito M, Morita Y, Ushiki T & Tamiya E (2002) Atomic force microscope-based dissection of human metaphase chromosomes and high resolutional imaging by carbon nanotube tip. *Arch Histol Cytol* **65**, 473–479.
47 Ushiki T & Hoshi O (2008) Atomic force microscopy for imaging human metaphase chromosomes. *Chromosome Res* **16**, 383–396.
48 Greenleaf WJ, Woodside MT & Block SM (2007) High-resolution, single-molecule measurements of biomolecular motion. *Annu Rev Biophys Biomol Struct* **36**, 171–190.
49 Neuman KC & Nagy A (2008) Single-molecule force spectroscopy: optical tweezers, magnetic tweezers and atomic force microscopy. *Nat Methods* **5**, 491–505.
50 Smith SB, Finzi L & Bustamante C (1992) Direct mechanical measurements of the elasticity of single DNA molecules by using magnetic beads. *Science* **258**, 1122–1126.
51 Strick TR, Allemand JF, Bensimon D, Bensimon A & Croquette V (1996) The elasticity of a single supercoiled DNA molecule. *Science* **271**, 1835–1837.
52 Leuba SH, Karymov MA, Tomschik M, Ramjit R, Smith P & Zlatanova J (2003) Assembly of single

chromatin fibers depends on the tension in the DNA molecule: magnetic tweezers study. *Proc Natl Acad Sci U S A* **100**, 495–500.
53 Bancaud A, Conde e Silva N, Barbi M, Wagner G, Allemand JF, Mozziconacci J, Lavelle C, Croquette V, Victor JM, Prunell A *et al.* (2006) Structural plasticity of single chromatin fibers revealed by torsional manipulation. *Nat Struct Mol Biol* **13**, 444–450.
54 Bancaud A, Wagner G, Conde ESN, Lavelle C, Wong H, Mozziconacci J, Barbi M, Sivolob A, Le Cam E, Mouawad L *et al.* (2007) Nucleosome chiral transition under positive torsional stress in single chromatin fibers. *Mol Cell* **27**, 135–147.
55 Kruithof M, Chien FT, Routh A, Logie C, Rhodes D & van Noort J (2009) Single-molecule force spectroscopy reveals a highly compliant helical folding for the 30-nm chromatin fiber. *Nat Struct Mol Biol* **16**, 534–540.
56 Strick TR, Allemand JF, Bensimon D & Croquette V (1998) Behavior of supercoiled DNA. *Biophys J* **74**, 2016–2028.
57 Charvin G, Strick TR, Bensimon D & Croquette V (2005) Tracking topoisomerase activity at the single-molecule level. *Annu Rev Biophys Biomol Struct* **34**, 201–219.
58 Lipfert J, Kerssemakers JW, Jager T & Dekker NH (2010) Magnetic torque tweezers: measuring torsional stiffness in DNA and RecA-DNA filaments. *Nat Methods* **7**, 977–980.
59 Deufel C, Forth S, Simmons CR, Dejgosha S & Wang MD (2007) Nanofabricated quartz cylinders for angular trapping: DNA supercoiling torque detection. *Nat Methods* **4**, 223–225.
60 Lionnet T, Dawid A, Bigot S, Barre FX, Saleh OA, Heslot F, Allemand JF, Bensimon D & Croquette V (2006) DNA mechanics as a tool to probe helicase and translocase activity. *Nucleic Acids Res* **34**, 4232–4244.
61 Hopfner KP & Michaelis J (2007) Mechanisms of nucleic acid translocases: lessons from structural biology and single-molecule biophysics. *Curr Opin Struct Biol* **17**, 87–95.
62 Lionnet T, Spiering MM, Benkovic SJ, Bensimon D & Croquette V (2007) Real-time observation of bacteriophage T4 gp41 helicase reveals an unwinding mechanism. *Proc Natl Acad Sci U S A* **104**, 19790–19795.
63 Norcum MT, Warrington JA, Spiering MM, Ishmael FT, Trakselis MA & Benkovic SJ (2005) Architecture of the bacteriophage T4 primosome: electron microscopy studies of helicase (gp41) and primase (gp61). *Proc Natl Acad Sci U S A* **102**, 3623–3626.
64 Sung P & Klein H (2006) Mechanism of homologous recombination: mediators and helicases take on regulatory functions. *Nat Rev Mol Cell Biol* **7**, 739–750.
65 Veaute X, Jeusset J, Soustelle C, Kowalczykowski SC, Le Cam E & Fabre F (2003) The Srs2 helicase prevents recombination by disrupting Rad51 nucleoprotein filaments. *Nature* **423**, 309–312.
66 Dupaigne P, Lavelle C, Justome A, Lafosse S, Mirambeau G, Lipinski M, Pietrement O & Le Cam E (2008) Rad51 polymerization reveals a new chromatin remodeling mechanism. *PLoS ONE* **3**, e3643.
67 Zaitseva EM, Zaitsev EN & Kowalczykowski SC (1999) The DNA binding properties of Saccharomyces cerevisiae Rad51 protein. *J Biol Chem* **274**, 2907–2915.
68 Dupaigne P, Le Breton C, Fabre F, Gangloff S, Le Cam E & Veaute X (2008) The Srs2 helicase activity is stimulated by Rad51 filaments on dsDNA: implications for crossover incidence during mitotic recombination. *Mol Cell* **29**, 243–254.
69 Arata H, Dupont A, Mine-Hattab J, Disseau L, Renodon-Corniere A, Takahashi M, Viovy JL & Cappello G (2009) Direct observation of twisting steps during Rad51 polymerization on DNA. *Proc Natl Acad Sci U S A* **106**, 19239–19244.
70 Mine J, Disseau L, Takahashi M, Cappello G, Dutreix M & Viovy JL (2007) Real-time measurements of the nucleation, growth and dissociation of single Rad51-DNA nucleoprotein filaments. *Nucleic Acids Res* **35**, 7171–7187.
71 van der Heijden T, Seidel R, Modesti M, Kanaar R, Wyman C & Dekker C (2007) Real-time assembly and disassembly of human RAD51 filaments on individual DNA molecules. *Nucleic Acids Res* **35**, 5646–5657.
72 Dame RT (2005) The role of nucleoid-associated proteins in the organization and compaction of bacterial chromatin. *Mol Microbiol* **56**, 858–870.
73 Lavelle C (2007) Transcription elongation through a chromatin template. *Biochimie* **89**, 516–527.
74 Workman JL (2006) Nucleosome displacement in transcription. *Genes Dev* **20**, 2009–2017.
75 Javaid S, Manohar M, Punja N, Mooney A, Ottesen JJ, Poirier MG & Fishel R (2009) Nucleosome remodeling by hMSH2-hMSH6. *Mol Cell* **36**, 1086–1094.
76 Grigoriev M & Hsieh P (1998) Migration of a Holliday junction through a nucleosome directed by the E. coli RuvAB motor protein. *Mol Cell* **2**, 373–381.
77 Eggleston AK, O'Neill TE, Bradbury EM & Kowalczykowski SC (1995) Unwinding of nucleosomal DNA by a DNA helicase. *J Biol Chem* **270**, 2024–2031.
78 Ramsperger U & Stahl H (1995) Unwinding of chromatin by the SV40 large T antigen DNA helicase. *EMBO J* **14**, 3215–3225.
79 Bouchiat C, Wang MD, Allemand J, Strick T, Block SM & Croquette V (1999) Estimating the persistence length of a worm-like chain molecule from force-extension measurements. *Biophys J* **76**, 409–413.

80 Lia G, Praly E, Ferreira H, Stockdale C, Tse-Dinh YC, Dunlap D, Croquette V, Bensimon D & Owen-Hughes T (2006) Direct observation of DNA distortion by the RSC complex. *Mol Cell* **21**, 417–425.
81 Allemand JF, Cocco S, Douarche N & Lia G (2006) Loops in DNA: an overview of experimental and theoretical approaches. *Eur Phys J E Soft Matter* **19**, 293–302.
82 Zhang Y, Smith CL, Saha A, Grill SW, Mihardja S, Smith SB, Cairns BR, Peterson CL & Bustamante C (2006) DNA translocation and loop formation mechanism of chromatin remodeling by SWI/SNF and RSC. *Mol Cell* **24**, 559–568.
83 Sirinakis G, Clapier CR, Gao Y, Viswanathan R, Cairns BR & Zhang Y (2011) The RSC chromatin remodelling ATPase translocates DNA with high force and small step size. *EMBO J* **30**, 2364–2372.
84 Shundrovsky A, Smith CL, Lis JT, Peterson CL & Wang MD (2006) Probing SWI/SNF remodeling of the nucleosome by unzipping single DNA molecules. *Nat Struct Mol Biol* **13**, 549–554.
85 Lorch Y, Zhang M & Kornberg RD (2001) RSC unravels the nucleosome. *Mol Cell* **7**, 89–95.
86 Saha A, Wittmeyer J & Cairns BR (2002) Chromatin remodeling by RSC involves ATP-dependent DNA translocation. *Genes Dev* **16**, 2120–2134.
87 Lorch Y, Cairns BR, Zhang M & Kornberg RD (1998) Activated RSC-nucleosome complex and persistently altered form of the nucleosome. *Cell* **94**, 29–34.
88 Shukla MS, Syed SH, Montel F, Faivre-Moskalenko C, Bednar J, Travers A, Angelov D & Dimitrov S (2010) Remosomes: RSC generated non-mobilized particles with approximately 180 bp DNA loosely associated with the histone octamer. *Proc Natl Acad Sci U S A* **107**, 1936–1941.
89 Bazett-Jones DP, Cote J, Landel CC, Peterson CL & Workman JL (1999) The SWI/SNF complex creates loop domains in DNA and polynucleosome arrays and can disrupt DNA-histone contacts within these domains. *Mol Cell Biol* **19**, 1470–1478.
90 Montel F, Fontaine E, St-Jean P, Castelnovo M & Faivre-Moskalenko C (2007) Atomic force microscopy imaging of SWI/SNF action: mapping the nucleosome remodeling and sliding. *Biophys J* **93**, 566–578.
91 Wang H, Bash R, Yodh JG, Hager G, Lindsay SM & Lohr D (2004) Using atomic force microscopy to study nucleosome remodeling on individual nucleosomal arrays in situ. *Biophys J* **87**, 1964–1971.
92 Schnitzler GR, Cheung CL, Hafner JH, Saurin AJ, Kingston RE & Lieber CM (2001) Direct imaging of human SWI/SNF-remodeled mono- and polynucleosomes by atomic force microscopy employing carbon nanotube tips. *Mol Cell Biol* **21**, 8504–8511.
93 Bouazoune K, Miranda TB, Jones PA & Kingston RE (2009) Analysis of individual remodeled nucleosomes reveals decreased histone-DNA contacts created by hSWI/SNF. *Nucleic Acids Res* **37**, 5279–5294.
94 Praly E (2009) Etude du mécanisme d'action des facteurs de remodelage de la chromatine, à l'échelle de la molécule unique. PhD thesis, Paris 7 – Denis Diderot, Paris.
95 de Cian A, Praly E, Dong F, Singh V, Pietrement O, Lavelle C, Croquette V, Le Cam E & Bensimon D (submitted) ATP-independent cooperative binding of yeast Isw1a to bare and nucleosomal DNA.
96 Yamada K, Frouws TD, Angst B, Fitzgerald DJ, DeLuca C, Schimmele K, Sargent DF & Richmond TJ (2011) Structure and mechanism of the chromatin remodelling factor ISW1a. *Nature* **472**, 448–453.
97 Claudet C, Angelov D, Bouvet P, Dimitrov S & Bednar J (2005) Histone octamer instability under single molecule experiment conditions. *J Biol Chem* **280**, 19958–19965.
98 Cui Y & Bustamante C (2000) Pulling a single chromatin fiber reveals the forces that maintain its higher-order structure. *Proc Natl Acad Sci U S A* **97**, 127–132.
99 Roopa T & Shivashankar GV (2006) Direct measurement of local chromatin fluidity using optical trap modulation force spectroscopy. *Biophys J* **91**, 4632–4637.
100 Kanger JS, Subramaniam V & van Driel R (2008) Intracellular manipulation of chromatin using magnetic nanoparticles. *Chromosome Res* **16**, 511–522.
101 de Vries AH, Krenn BE, van Driel R, Subramaniam V & Kanger JS (2007) Direct observation of nanomechanical properties of chromatin in living cells. *Nano Lett* **7**, 1424–1427.
102 Lavelle C & Buckle M (2009) Nucleic acid-protein interactions: wedding for love or circumstances? *Biochimie* **91**, 943–950.